

UC Irvine

UC Irvine Previously Published Works

Title

Flow-independent Nitric Oxide Exchange Parameters in Cystic Fibrosis

Permalink

<https://escholarship.org/uc/item/2mh2v3qh>

Journal

American Journal of Respiratory and Critical Care Medicine, 165(3)

ISSN

1073-449X

Authors

SHIN, HYE-WON

ROSE-GOTTRON, CHRISTINE M

SUFI, RAMINDRJIT S

et al.

Publication Date

2002-02-01

DOI

10.1164/ajrccm.165.3.2105098

Copyright Information

This work is made available under the terms of a Creative Commons Attribution License, available at <https://creativecommons.org/licenses/by/4.0/>

Peer reviewed

Flow-independent Nitric Oxide Exchange Parameters in Cystic Fibrosis

HYE-WON SHIN, CHRISTINE M. ROSE-GOTTRON, RAMINDRIT S. SUFI, FEDERICO PEREZ, DAN M. COOPER, ARCHIE F. WILSON, and STEVEN C. GEORGE

Department of Chemical Engineering and Materials Science, Center for Biomedical Engineering, Department of Pediatrics, The General Clinical Research Center, Department of Medicine, Division of Pulmonary and Critical Care, University of California, Irvine, Irvine; and Miller Children's Hospital at Long Beach Memorial Medical Center, Long Beach, California

Exhaled nitric oxide (NO) remains a promising noninvasive index for monitoring inflammatory lung diseases; however, the plateau concentration ($C_{NO,plat}$) is nonspecific and requires a constant exhalation flow rate. We utilized a new technique that employs a variable flow rate to estimate key flow-independent parameters characteristic of NO exchange in a group ($n = 9$) of 10 to 14 yr-old healthy children and children with cystic fibrosis (CF): maximum flux of NO from the airways ($J_{NO,max}$, $pl\ s^{-1}$), diffusing capacity of NO in the airways ($D_{NO,air}$, $pl\ s^{-1}\ ppb^{-1}$), steady-state alveolar concentration ($C_{alv,ss}$, ppb), and mean tissue concentration of NO in the airways ($\bar{C}_{tiss,air}$, ppb). We determined the following mean (\pm SD) values in the healthy children and patients with CF for $J_{NO,max}$, $D_{NO,air}$, $C_{alv,ss}$, and $\bar{C}_{tiss,air}$ respectively: 784 ± 465 and $607 \pm 648\ pl\ s^{-1}$; 4.82 ± 3.07 and $17.6 \pm 12.1\ pl\ s^{-1}\ ppb^{-1}$; 4.63 ± 3.59 and $1.96 \pm 1.18\ ppb$; and 198 ± 131 and $38 \pm 25\ ppb$. $D_{NO,air}$ is elevated ($p = 0.007$), and both $C_{alv,ss}$ and $\bar{C}_{tiss,air}$ are reduced ($p = 0.05$ and 0.002 , respectively) in CF. In contrast, $C_{NO,plat}$ for healthy control subjects and patients with CF are not statistically different at both exhalation flow rates of 50 ml/s (17.5 ± 11.5 and 11.5 ± 8.97) and at 250 ml/s (7.11 ± 5.36 and 4.28 ± 3.43). We conclude that $D_{NO,air}$, $\bar{C}_{tiss,air}$, and $C_{alv,ss}$ may be useful noninvasive markers of CF.

Keywords: nitric oxide; parameter estimation; airways; inflammation; healthy children

Nitric oxide (NO) is an important endogenous mediator that arises from the airways and alveoli and can be detected in the exhaled breath (1, 2). Several inflammatory disorders, such as asthma, are associated with elevated exhaled NO concentrations (3–7). Although plateau NO concentration ($C_{NO,plat}$) in patients with cystic fibrosis (CF), a congenital lung disease marked by inflammation, has been reported to be decreased (7–9), it has also been reported to be unchanged (5, 6, 10–13) when compared with healthy control subjects. These paradoxical results for CF can be explained potentially by both real alterations in the underlying physiology due to differences in disease penetration, duration of disease, types of colonizing organisms, and the coexistence of atopy or asthma, as well as differences in the experimental protocol (e.g., variation in exhalation flow rate) (14, 15).

$C_{NO,plat}$ may not be a specific or sensitive indicator of NO exchange dynamics in CF, because in and of itself, $C_{NO,plat}$ provides little or no anatomic information. We have recently described a new, simple, and robust technique that utilizes a pre-

expiratory 20-s breathhold followed by decreasing flow rate (~ 6 –1% vital capacity/s) maneuver to simultaneously determine several key flow-independent parameters that could reveal underlying physiological mechanisms (16): maximum flux of NO from the airways ($J_{NO,max}$, $pl\ s^{-1}$), diffusing capacity of NO in the airways ($D_{NO,air}$, $pl\ s^{-1}\ ppb^{-1}$), steady-state alveolar concentration ($C_{alv,ss}$, ppb), and mean (over radial position) concentration of NO within the tissue phase ($\bar{C}_{tiss,air}$, ppb, equal to the ratio $J_{NO,max}/D_{NO,air}$). These provide potentially useful and reproducible information regarding net production and diffusion of NO in the airways and alveolar regions of the lungs. Thus, by providing a more detailed description of the NO exchange dynamics throughout the lung, we hypothesize that this new technique will distinguish NO exchange dynamics in patients with CF from healthy children.

METHODS

Subjects

Nine healthy children and nine children with previously diagnosed CF (ages 10–14) participated in this study. Subjects were categorized as healthy on the basis of standard spirometry ($FEV_1 > 75\%$ of predicted on the basis of their race, age, and height) and no clinical history of chronic lung disease. Subject characteristics are presented in Table 1 including details of their clinical history. The Institutional Review Board at the University of California, Irvine approved the protocol, and informed consent was obtained from subjects and parents.

Experimental Protocol

Forced vital capacity (FVC) and forced expiratory volume in 1 s (FEV_1) were measured in all subjects (V_{max229} ; SensorMedics, Yorba Linda, CA) by using the best performance (see Table 1) from three consecutive maneuvers before measuring the indices of NO exchange dynamics.

Each subject performed two types of exhalation maneuvers: (1) vital capacity maneuvers in triplicate at a constant exhalation flow of ~ 50 ml/s and ~ 250 ml/s according to the ATS (American Thoracic Society) and the ERS (European Respiratory Society) (17, 18) to determine $C_{NO,plat}$ without breathhold; (2) five repetitions of a 20-s preexpiratory breathhold followed by a decreasing flow rate maneuver (16). During the breathhold, a positive pressure of > 5 cm H_2O was maintained to prevent nasal contamination (17). A schematic of the experimental apparatus has been previously presented (16). After the breathhold, the exhalation valve was opened allowing the patient to expire. The expiratory flow rate progressively decreased during the exhalation from 6% to 1% of vital capacity per second using a Starling resistor (Hans Rudolph Inc., Kansas City, MO) with a variable resistance.

Airstream Analysis

A chemiluminescence NO analyzer (NOA280; Sievers, Inc., Boulder, CO) was used to measure the exhaled NO concentration. The instrument was calibrated on a daily basis using a certified NO gas (45 ppm in N_2 ; Sievers, Inc.). The zero point calibration was performed with an NO filter (Sievers, Inc.) and done immediately before the collection of a profile. The flow rate and pressure signals were measured using a pneumotachometer (RSS100; Hans Rudolph Inc.). The pneumotachometer

(Received in original form May 21, 2001; accepted in final form October 30, 2001)

Supported by grants from the National Institutes of Health (R29-HL60636, HD23969, and M01RR00827-S1).

Correspondence and requests for reprints should be addressed to Steven C. George, M.D., Ph.D., Department of Chemical Engineering and Materials Science, 916 Engineering Tower, University of California, Irvine, Irvine, CA 92697-2575. E-mail: scgeorge@uci.edu

Am J Respir Crit Care Med Vol 165. pp 349–357, 2002

DOI: 10.1164/rccm.2105098

Internet address: www.atsjournals.org

TABLE 1. PHYSICAL CHARACTERISTICS OF SUBJECTS

Subject	Sex	Age (yr)	Hgt (in)	Wgt (lb)	lwgt (lb)	V _{air} (ml)	FVC		FEV ₁		FEV ₁ /FVC
							(L)	(% pred)	(L)	(% pred)	
(A) Healthy Children											
1	F	13	63	134	123	136	2.88	94	2.55	94	95
2	F	11	58	97	108	119	2.93	112	2.54	115	94
3	M	11	59	115	119	130	3.05	111	2.55	106	84
4	M	12	60	88	122	134	2.79	98	2.22	90	81
5	F	11	63	129	124	135	3.78	121	3.02	115	81
6	M	12	65	161	141	153	4.11	122	3.43	117	83
7	F	10	55	75	98	108	2.34	103	1.96	100	87
8	F	14	63	106	123	137	3.35	107	2.70	97	83
9	M	12	61	119	126	138	3.06	103	2.44	94	80
Mean		12	61	114	120	132	3.14	108	2.6	103	85
(B) Patients with Cystic Fibrosis											
1	M	10	56	68	109	119	2.44	99	2.15	99	88
2	F	11	59	90	161	172	3.05	113	2.42	106	80
3	M	14	67	111	147	161	3.42	82	2.62	73	78
4	F	10	53	63	91	101	1.59	77	1.28	72	82
5	F	13	57	81	106	119	1.61	63	1.38	61	86
6	F	10	52	61	86	96	1.65	88	1.46	89	89
7	M	14	63	103	134	148	2.36	64	1.89	60	80
8	F	13	56	80	100	113	1.58	67	1.04	49	66
9	F	12	57	69	103	115	1.50	63	1.03	49	71
Mean		12	58	81*	115	128	2.2*	82*	1.8*	76*	81

(C) Clinical History of the Patients with Cystic Fibrosis

Subject	Genotype	Diagnosis	Penetration	Organisms	Atopy	RAD	Therapies
1	Δf508 2789 + 56-A	21 mo	Mild lung disease ABPA, sinus	SA STENO	Yes	Yes	Albuterol, intal, enzymes, DNase, motrin, inhaled str
2	Δf508	Fetus	Sinus	SA, PSA	Yes	Yes	Albuterol, intal, enzymes, DNase, tobi, nasal str, inhaled str
3	Δf508	1989	Sinus	PSA	Yes	—	Albuterol, intal, enzymes, DNase, tobi, nasal str
4	Δf508	1990	Sinus	SA, PSA	Yes	Yes	Albuterol, intal, enzymes, DNase, tobi, nasal str, inhaled str
5	Δf508	1990	Sinus	SA, PSA	Yes	Yes	Albuterol, intal, enzymes, DNase, tobi, nasal str, inhaled str
6	Δf508	1993	Sinus	PSA, MRSA	Yes	Yes	Albuterol, intal, enzymes, DNase, tobi, nasal str, inhaled str
7	g542x	1996	Hypersplenism, FTT, Dm, sinus, hemoptysis, thrombocytopenia	SA, STENO	Yes	—	Albuterol, intal, enzymes, DNase, nasal str, insulin, actigal
8	Δf508	1996	Moderate lung disease, ABPA GTUBE, sinus, FTT	PSAM, PSANM	Yes	Yes	Albuterol, intal, enzymes, DNase, tobi, nasal str, inhaled str
9	—	—	Severe lung disease, sinus FTT, hemoptysis	SA, PSA	Yes	Yes	Albuterol, intal, enzymes, DNase, tobi, nasal str, inhaled str

Definition of abbreviations: ABPA = allergic bronchopulmonary aspergillosis; Dm = diabetes mellitus; FEV₁ = forced expiratory volume in 1 s; FVC = forced vital capacity; FTT = failure to thrive; GTUBE = gastrostomy tube; Hgt = height; lwgt = ideal body weight; MRSA = methacillin-resistant *Staphylococcus aureus*; PSA = *Pseudomonas* species; PSAM = *Pseudomonas aeruginosa* mucoid strain; PSANM = *Pseudomonas aeruginosa* nonmucoid strain; RAD = reactive airways disease; SA = *Staphylococcus aureus*; STENO = *Stenotrophomonas maltophilia*; str = steroid; Wgt = body weight.

* Statistically different from healthy control subjects (t test with α < 0.05).

was calibrated daily and was set to provide the flow in units of STPD and pressure in units of mm Hg.

Parameter Estimation and Data Analysis

A previously described two-compartment model was used to estimate the four key flow-independent parameters in healthy children and patients with CF (16, 19). Only three of the four parameters are independent, as C_{tiss,air} is the ratio of two of the other parameters, maximum total volumetric flux per unit airway volume (pl/s) of NO from the airway wall (J_{no,max})/diffusing capacity (pl s⁻¹ ppb⁻¹) of NO in the

airways (D_{no,air}). Figure 1 is a simple schematic of the two-compartment model and flow-independent parameters. Mathematical estimation of the parameters (C_{alv,ss}, D_{no,air}, J_{no,max}) has been previously described in detail (16), and is accomplished by nonlinear least-square minimization utilizing a conjugated direction minimization algorithm.

The alveolar region is characterized by the steady-state alveolar concentration, C_{alv,ss} (19, 20). Upon exhalation, the air passes through the airway tree and additional NO is transferred from the airway tissue. This additional volume of NO is referred to as the flux of NO from the airways, volumetric flux of NO (J_{no}) (pl/s), and is not a constant, but a linear function of the gas phase concentration (19, 21, 22):

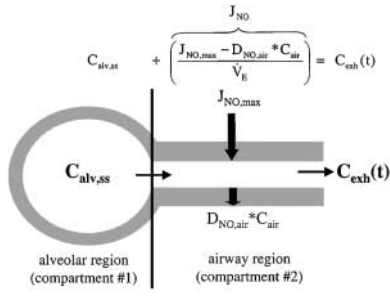


Figure 1. Schematic of two-compartment model used to describe NO exchange dynamics. Exhaled NO concentration, C_{exh} is the sum of two contributions—the alveolar region and the airway region—which depends on three flow-independent parameters: maximum total volumetric flux of NO from the airway wall ($J_{NO,max}$, $pl\ s^{-1}$), diffusing capacity of NO in the airways ($D_{NO,air}$, $pl\ s^{-1}\ ppb^{-1}$), and steady-state alveolar concentration ($C_{alv,ss}$, ppb). J_{NO} is the total flux (pl/s) of NO between the tissue and gas phase in the airway, and inversely depends on the residence time of a gas bolus and thus the exhalation flow rate, \dot{V}_E . The expression presented for J_{NO} is valid for exhalation flows larger than approximately 1% of the vital capacity per second.

$$J_{NO} = J_{NO,max} - D_{NO,air} C_{air} \quad (1)$$

Thus, airway compartment is not well mixed, but the concentration depends on the axial or longitudinal direction and is characterized by two parameters: $J_{NO,max}$ and $D_{NO,air}$. $J_{NO,max}$ is the maximum flux of NO

from the airway tissue, which is equal to the airway compartment flux if the gas phase concentration, concentration (ppb) of NO in the airway compartment (C_{air}), were zero.

An alternative presentation of the three flow-independent parameters includes the use of the mean (over radial position) tissue concentration in the airways, $\bar{C}_{tiss,air}$, instead of $J_{NO,max}$ (22). $\bar{C}_{tiss,air}$ is simply the ratio $J_{NO,max}/D_{NO,air}$. This is more easily demonstrated by expressing J_{NO} in an alternate but equivalent form to Equation 1 (16, 21, 22):

$$J_{NO} = J_{NO,air} (\bar{C}_{tiss,air} - C_{air}) \quad (2)$$

Note that $J_{NO,max}$ is simply the product $D_{NO,air} \cdot \bar{C}_{tiss,air}$. In Equation 2, J_{NO} is expressed as proportional to the appropriate concentration difference between the airway tissue ($\bar{C}_{tiss,air}$) and the gas stream (C_{air}). The coefficient of proportionality is $D_{NO,air}$. Thus, $D_{NO,air}$ can be interpreted as a conductance for mass transfer of NO between the airway tissue and the gas phase.

Figures 2A (healthy) and 2C (CF) are representative experimental exhalation profiles as well as the model simulation. Figures 2B (healthy) and 2D (CF) are the corresponding exhaled volume, flow, and pressure tracings. The model does not predict phase I and II of the exhalation profile, where the accumulated NO during breathholding in the conducting airways and transition region of the lungs exits the mouth. This discrepancy is attributed to axial diffusion that our model neglects. Although the precise shape of phase I cannot be accurately simulated with the model, the absolute amount of NO in phase I and II can be predicted. Thus, our technique utilizes the information

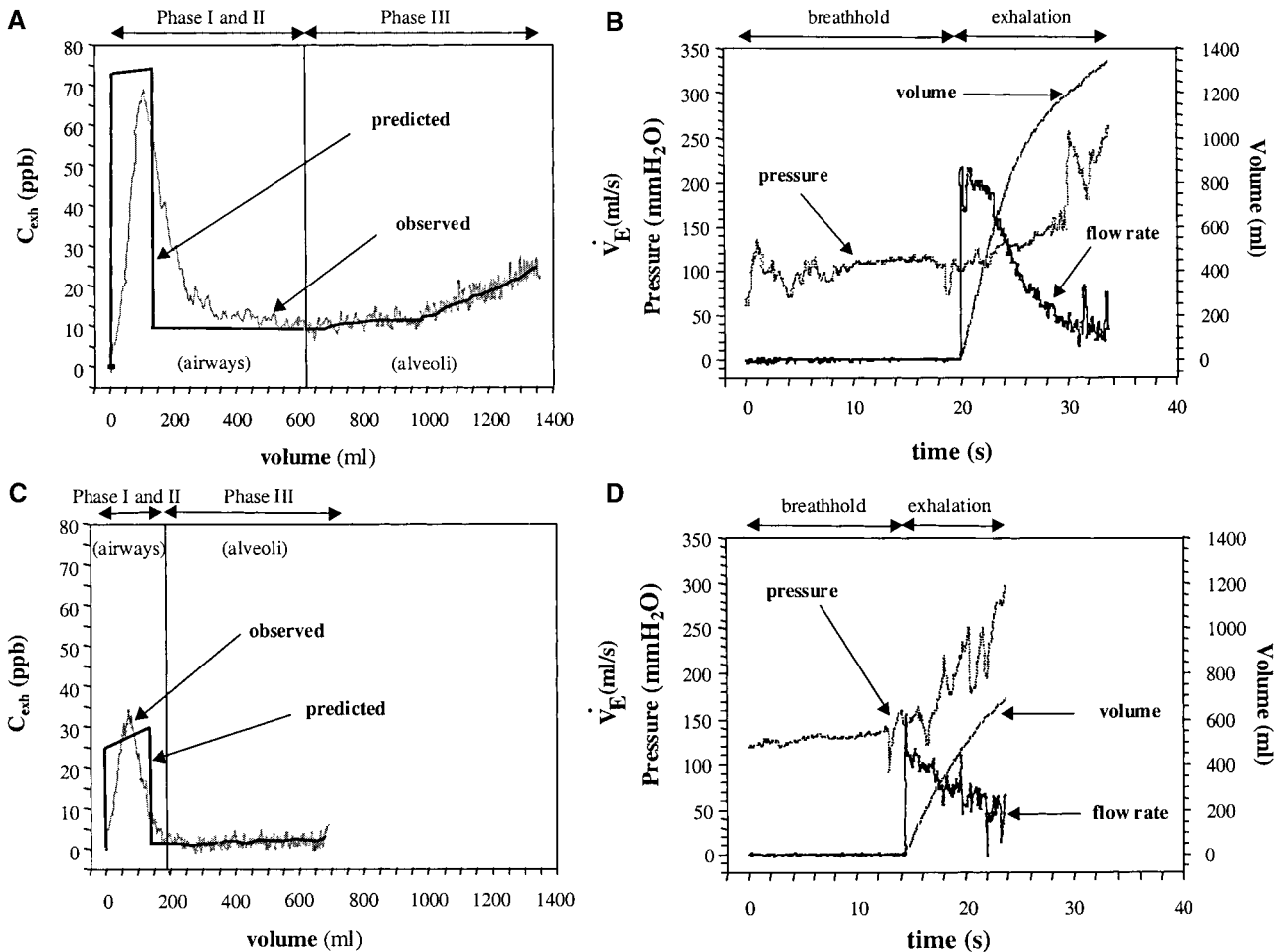


Figure 2. Representative exhaled NO concentration profiles (*dashed lines*) and model fit (*dark line*) utilizing the 20-s preexpiratory breathhold followed by a decreasing flow rate maneuver are shown as a function of exhaled volume for healthy child (A) and a patient with CF (C). In addition, the corresponding exhalation flow rate, exhaled volume, and pressure tracings during the exhalation are also presented as a function of time for the healthy child (B) and the patient with CF (D). Flow rates are controlled at ~ 6–1% of the each subject’s vital capacity per second, and > 5 cm H₂O of pressure is maintained through the breathing maneuver. Detailed description of parameters and regression techniques are described in the text and Appendix.

from phase I and II by forcing the model to simulate the total amount of NO eliminated in phase I and II (area under the curve as depicted in Figures 2A and 2C) of the exhalation in addition to simulating the precise exhaled concentration (ppb) (C_{exh}) over phase III. To ensure complete emptying of the airway compartment after breathhold, we define the transition from phase II and III as the point in the exhalation for which the slope (dC_{exh}/dV) of the exhalation profile is zero.

We assessed the ability of the model to simulate the profile by comparing the area under the curve in phase I and II in the experimental and theoretical data. Figure 3 presents the percentage of the experimental area under the curve predicted by the model for all 45 breathing maneuvers (nine subjects times five repeated maneuvers). It is evident that there are a few outliers (solid circles, < 80% of the experimental area under the curve) in each population, which represent profiles that the two-compartment model cannot adequately simulate. These profiles were subsequently discarded. There were no more than two discarded profiles from any individual subject. Thus, the population mean values for each of the parameters for the healthy children and patients with CF are based on exhalation profiles in which the model-predicted area under the curve for phase I and II is > 80% of the experimental area under the curve.

The intramaneuver (superscript m), intrasubject (superscript s), and intrapopulation (superscript p) variability have been described previously (16), and will be characterized by the 95% confidence interval expressed as a percentage of the estimated parameter value, intramaneuver $100(1-\alpha)\%$ confidence interval (CI^m), intrasubject $100(1-\alpha)\%$ confidence interval (CI^s), and intrapopulation $100(1-\alpha)\%$ confidence interval (CI^p), respectively. $C_{\text{NO,plat}}$ and the flow-independent parameters are expressed as a mean and 95% confidence interval (CI). To determine the relation between pulmonary function (FVC and FEV_1/FVC) and the estimated three flow-independent parameters, linear regression and correlation were performed. A p value of < 0.05 is considered significant.

RESULTS

FVC, FEV_1 , FEV_1/FVC , and the clinical history of the CF subjects are presented in Table 1. Seven of the nine subjects with CF had concurrent reactive airways diseases, and all of these subjects were currently taking inhaled corticosteroids. The two subjects who did not have reactive airways disease were taking only nasal corticosteroids. FVC and FEV_1 were significantly lower in CF than in healthy children ($p < 0.05$). Means for each of the nine subjects in each category and the population mean are presented in Figure 4. In the nine children with CF, only six were able to complete the 20-s breathhold. In the three children who were not able to hold their breath for 20 s, one held their breath for 15 s, and two for 10 s. Estimated $J_{\text{NO,max}}$ is not significantly different between healthy control subjects and patients with CF ($p = 0.52$); however, $D_{\text{NO,air}}$ is significantly elevated ($p = 0.007$) and $C_{\text{alv,ss}}$ and $\bar{C}_{\text{tiss,air}}$ are significantly reduced ($p = 0.05$ and 0.002 , respectively) in CF.

Mean values for CI^p for healthy children and CF are 46% and 82%, 49% and 53%, 60% and 46%, and 51% and 51% for $J_{\text{NO,max}}$, $D_{\text{NO,air}}$, $C_{\text{alv,ss}}$, and $\bar{C}_{\text{tiss,air}}$, respectively. Thus, the varia-

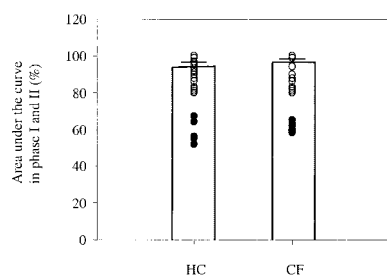


Figure 3. Absolute amount of NO eliminated in phase I and II of the exhalation profile as predicted by the model is shown as a percentage of the NO eliminated experimentally. Each circle represents one of the 45 individual data points from the individual breathing maneuvers. Solid circles indicate outliers (model predicted is

< 80% of experimentally measured), and means with 95% confidence interval are calculated after elimination of the outliers.

tion across the population of healthy children and patients with CF is approximately the same for each of the parameters.

The population means of CI^m and CI^s for each parameter are presented in Figure 5 for the healthy control subjects and patients with CF. $J_{\text{NO,max}}$ and $C_{\text{alv,ss}}$ for healthy controls are estimated with high accuracy (population mean $CI^m = 38\%$ and 97% , respectively) relative to $D_{\text{NO,air}}$ (population mean $CI^m = 128\%$). For CF, the population mean for CI^m for the three flow-independent parameters are 118%, 167%, and 284% for $J_{\text{NO,max}}$, $D_{\text{NO,air}}$, and $C_{\text{alv,ss}}$, respectively, which are much larger than the healthy children. In contrast to CI^m , population mean values for CI^s for each of the parameters are not statistically different between healthy control subjects and patients with CF, and range from 26% to 65% (Figure 5).

None of the flow-independent parameters had any significant correlation with standard indices of lung volume (FVC) or airway obstruction (FEV_1/FVC) for both healthy children and patients with CF.

Mean $C_{\text{NO,plat}}$ (\pm CI) from the experimental maneuvers were 20.2 ± 10.1 ppb and 10.2 ± 3.97 ppb for healthy children and 8.91 ± 5.38 ppb and 4.79 ± 2.48 ppb for patients with CF at the target flow rates of ~ 50 ml/s and ~ 250 ml/s, respectively. The experimental values for each of the individuals are presented in Table 2 with model-predicted $C_{\text{NO,plat}}$ in parenthesis. $C_{\text{NO,plat}}$ at the targeted flow rate of 50 ml/s and 250 ml/s are lower for patients with CF when compared with healthy control subjects; however, the mean exhalation flow rates for patients with CF were larger in both cases (Table 2). Because a larger flow rate will decrease $C_{\text{NO,plat}}$, one must attempt to control for this confounding variable. We used the estimated flow-independent parameters for each of the subjects to estimate $C_{\text{NO,plat}}$ using the two-compartment model (see governing equation in the Appendix) at precisely an exhalation flow rate of 50 and 250 ml/s (Table 2). Mean $C_{\text{NO,plat}}$ (\pm CI) from the model were 17.5 ± 8.97 ppb and 7.11 ± 4.03 ppb for healthy children and 11.5 ± 6.89 ppb and 4.28 ± 2.64 ppb for patients with CF at 50 ml/s and 250 ml/s, respectively. The model-predicted $C_{\text{NO,plat}}$ are still lower for children with CF when compared with healthy children, but the difference is no longer significant ($p > 0.05$).

DISCUSSION

This study has estimated several flow-independent parameters characteristic of NO exchange dynamics in the lungs, which have not been measured in CF before, and compared these to the plateau concentration at a constant exhalation flow rate. When compared with healthy control subjects, we found differences in $C_{\text{NO,plat}}$ that were not significant if one controlled for differences in the exhalation flow rate. In contrast, the flow-independent parameters differed substantially between patients with CF and healthy control subjects. Thus, our new method provides greater sensitivity in distinguishing NO exchange dynamics between healthy control subjects and patients with CF.

The difference between $C_{\text{NO,plat}}$ and the flow-independent parameters is highlighted by examining the composite experimental and model-predicted exhalation profiles from the population of patients with CF and healthy control subjects (Figure 6). Figure 6A depicts the composite experimental profile for each population by taking the mean exhaled concentration at equivalent exhaled volumes. Figure 6B presents the composite model predicted profiles by using the average values for the flow-independent parameters in the model equation (see Appendix). It is evident that there are small changes in the exhaled NO concentration during phase III due to small changes

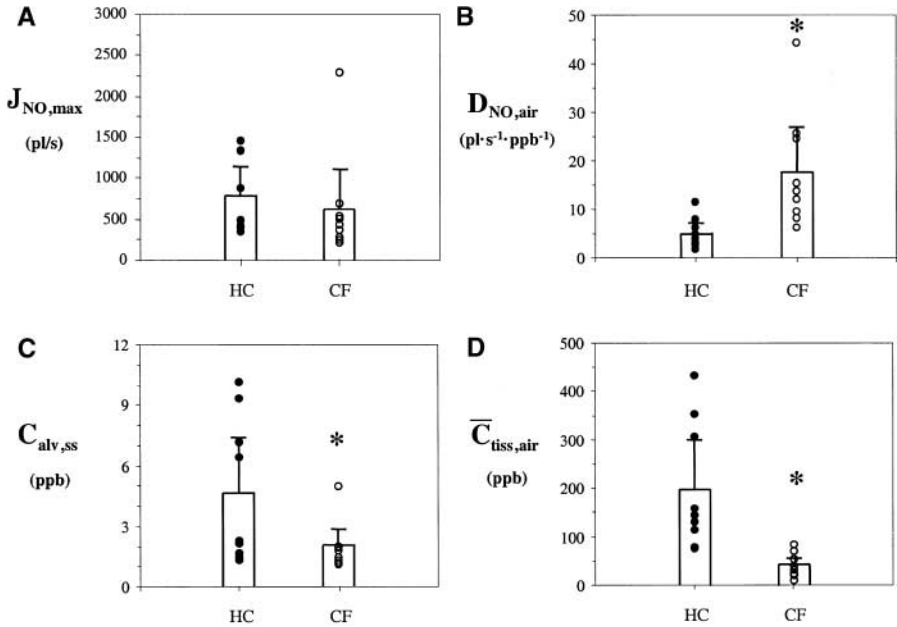


Figure 4. Population means for the four flow-independent parameters (A: $J_{NO,max}$, B: $D_{NO,air}$, C: $C_{alv,ss}$, D: $C_{tiss,air}$) of healthy control subjects and patients with CF are presented as a column with individual mean values for each of the nine subjects (solid circle: healthy control subjects, open circle: patients with CF) superimposed. Error bar indicates the intrapopulation 95% confidence interval (CI^p). *Statistically different from healthy control subjects ($p < 0.05$).

in $C_{alv,ss}$ and J_{NO} . However, there are very large differences in the concentration of NO in phase I and II in which the differences in NO exchange dynamics between healthy control subjects and patients with CF are magnified during a breathhold. The magnification of the airway compartment allows one to estimate $D_{NO,air}$, $J_{NO,max}$, and $C_{tiss,air}$, achieve more detailed information regarding NO exchange dynamics, and distinguish healthy children from patients with CF.

Interpreting the significant increase in $D_{NO,air}$ observed in patients with CF requires understanding the factors that affect its value. Thicker and more viscous mucus present in patients with CF would tend to increase the diffusion distance for NO as well as the “ease” at which NO can diffuse. Both of these observations would decrease $D_{NO,air}$ and contrast with our experimental observation of an elevated $D_{NO,air}$.

It has been previously hypothesized that inflammation may

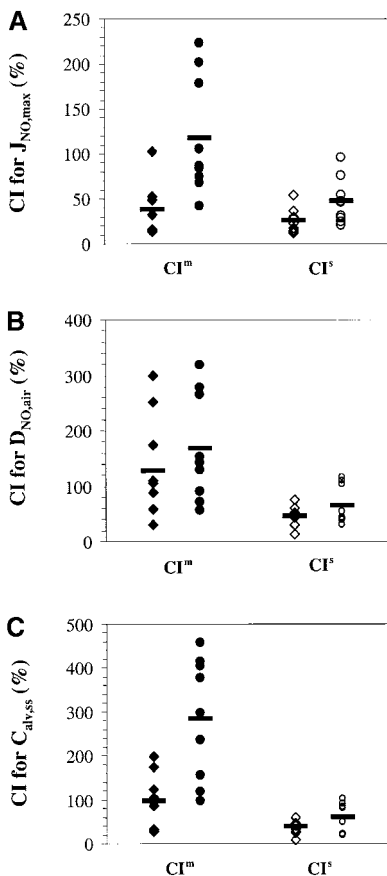


Figure 5. Mean values for each subject for intramaneuver (CI^m, closed symbols) and intrasubject (CI^s, open symbols) confidence intervals are shown for each parameter ($J_{NO,max}$, $D_{NO,air}$, and $C_{alv,ss}$) for healthy control subjects and patients with CF. Solid bar indicates population mean. ◆◇ HC; ●● CF.

TABLE 2. MODEL PREDICTED AND EXPERIMENTALLY OBTAINED $C_{NO,plat}$

Subject	$C_{NO,plat}, \dot{V}_E$ (Experimental Data [Model-Predicted])			$C_{NO,plat}$ (Model-Predicted)	
	ppb	ml/s	ppb	ml/s	
(A) Healthy Children					
1	14.4 (8.12)*	64.7	10.8 (6.19)	95.8	9.86
2	41.0 (36.2)	47.6	17.7 (18.1)	159	35.0
3	20.6 (19.5)	61.6	13.3 (12.7)	142	22.1
4	9.60 (8.53)	44.5	3.23 (2.74)	233	7.78
5	33.0 (30.0)	61.1	15.8 (15.3)	213	34.5
6	7.21 (5.63)	90.3	4.75 (3.68)	170	8.93
7	10.7 (9.52)	59.7	6.73 (6.33)	101	11.0
8	9.34 (8.61)	68.9	6.36 (5.72)	129	10.9
9	36.0 (33.1)	45.6	13.5 (12.3)	227	31.0
Mean	20.2 (17.7)	60.4	10.2 (9.23)	163	17.5
CI	10.1 (12.3)	10.9	3.97 (5.48)	39.9	8.97
(B) Children with Cystic Fibrosis					
1	7.70 (7.21)*	66.5	4.93 (3.79)	161	9.05
2	25.4 (23.3)	88.8	12.4 (12.8)	240	32.4
3	3.67 (4.45)	128	2.68 (3.02)	238	8.41
4	10.6 (10.5)	73.1	5.12 (4.39)	268	14.1
5	6.15 (6.35)	106	3.86 (4.03)	230	10.7
6	7.37 (5.30)	57.7	3.55 (2.89)	141	5.89
7	6.10 (6.66)	60.6	3.46 (4.62)	114	7.50
8	4.31 (5.61)	25.4	2.29 (2.78)	112	4.06
9	4.80 (5.24)	57.2	2.56 (3.19)	149	5.72
Mean	8.91† (8.29)	75.8	4.79† (4.61)	188	11.5
CI	5.38 (5.89)	24.3	2.48 (3.14)	48.2	6.89

Definition of abbreviations: CI = confidence interval; $C_{NO,plat}$ = plateau NO concentration; \dot{V}_E = volumetric flow rate of air during expiration.

* Model-predicted plateau NO concentrations at each constant flow rate are presented in parentheses.

† Statistically different from healthy control subjects (t test with $p < 0.05$)

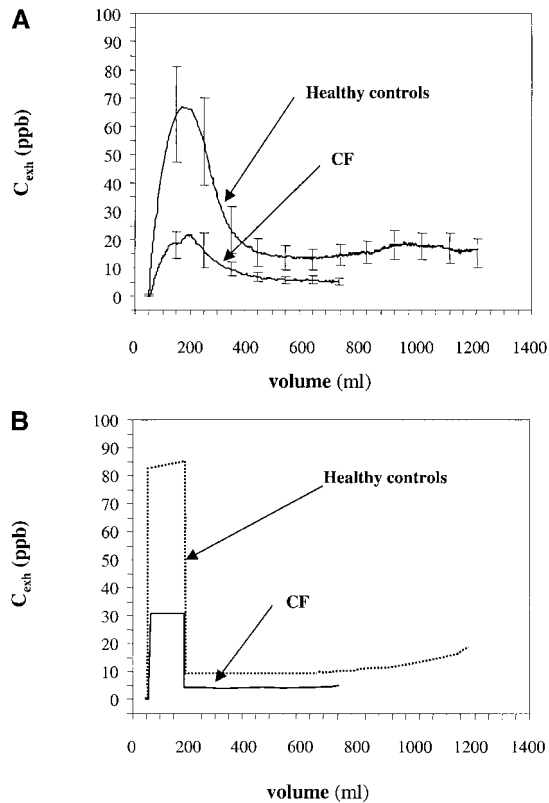


Figure 6. Composite experimental (A) and model-predicted (B) NO exhalation profiles are presented for the 20-s breathhold followed by a decreasing flow rate maneuver for healthy control subjects and patients with CF. Population mean values for the three parameters, $J_{NO,max}$, $D_{NO,air}$, and $C_{alv,ss}$ for healthy control subjects and children with CF were utilized in the model prediction and are equal to 784 and 607 $pl\ s^{-1}$, 4.82 and 17.6 $pl\ s^{-1}\ ppb^{-1}$, and 4.63 and 1.96 ppb, respectively. FVC was set equal to the mean value for each population, and the flow rate decreased from 6% to 1% of the vital capacity per second.

increase the surface area of the airways producing NO by stimulating the inducible form of nitric oxide synthase (iNOS) (34, 35). This would increase $D_{NO,air}$ (proportional to surface area, *see* Appendix), which is consistent with our observation; however, iNOS expression is reduced in epithelial cells from patients with CF even though levels of inflammatory mediators such as tumor necrosis factor (TNF)- α and interleukin (IL)-1 β are increased in bronchoalveolar lavage (36–38). Furthermore, neutrophils, which increase iNOS expression in normal cells, do not enhance the iNOS expression in CF epithelial cells (37).

The impact of chemical consumption of NO, as characterized by k (a first-order rate constant), is also a possibility. *In vivo*, NO reacts with several substrates including oxygen, protein thiols (e.g., glutathione), and superoxide. In CF, there are increased numbers of neutrophils, which can produce toxic radical species including superoxide. Normally, glutathione (GSH) provides an effective antioxidant role in the lung; however, in CF, the concentration of GSH has been reported to be decreased (23) as a result of abnormal GSH transport related to the defective CFTR (24). The presence of neutrophils and lower levels of GSH may provide an environment in which excess superoxide can react quickly with NO to form peroxynitrite and other more stable end products such as nitrite and nitrate (25, 26).

It has been postulated that the half life, $t_{1/2}$, *in vivo* in healthy control subjects is between the range of 0.1 to 10 s,

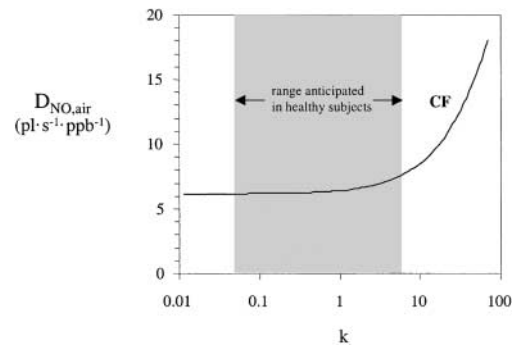


Figure 7. Predicted $D_{NO,air}$ (by Equation A2) is plotted as a function of reaction rate constant k . Values for A_{air} , $\lambda_{tiss,air}$, $D_{NO,tiss}$, and L_{tiss} are 9,100 cm^2 , 0.0412, 3.3×10^{-5} cm^2/s , and 0.01 cm, respectively, and are obtained from a previous study (28). The shaded region depicts that predicted for a healthy subject. Patients with CF may have a larger value for k as indicated.

which is equivalent to between 7 and 0.07 s^{-1} based on the simple relationship $k = \ln(2)/t_{1/2}$ (the shaded region of Figure 7). Figure 7 plots a theoretical estimate of $D_{NO,air}$ (*see* Appendix for details) as a function of k . $D_{NO,air}$ increases as k increases ($t_{1/2}$ decreases). The relationship is highly nonlinear: $D_{NO,air}$ is independent of k for $k < 1$, but becomes a strong positive function of k for $k > 10$. The positive relationship between $D_{NO,air}$ and k is due to an increase in the radial gradient of NO concentration from chemical consumption and is a well-known phenomenon in chemical reaction engineering (33).

The increase in chemical consumption of NO acts to increase $D_{NO,air}$, or the conductance for mass transfer, but would decrease the mean tissue concentration, $\bar{C}_{tiss,air}$. In addition, reduced iNOS expression would also tend to reduce $\bar{C}_{tiss,air}$. Thus, the effect on $D_{NO,air}$ and $\bar{C}_{tiss,air}$ would tend to negate each other in terms of the impact on the actual flux of NO (J_{NO} or $J_{NO,max}$, *see* Equations 1 and 2) from the airways. $C_{alv,ss}$ is reduced in patients with CF, but this represents only 17–24% of $C_{NO,plat}$ at an exhalation flow rate of 50 ml/s. This provides a potential explanation for why some studies on CF have reported no statistical change, or a small decrease in exhaled NO concentration, and why the flow-independent parameters are potentially more sensitive. A patient with CF could have highly elevated $D_{NO,air}$ but greatly reduced $\bar{C}_{tiss,air}$; thus, J_{NO} and $J_{NO,max}$ are near normal, and a decrease in $C_{alv,ss}$ results in a small decrease in $C_{NO,plat}$, which may not be detectable when compared with healthy control subjects (compare healthy subject #8 with CF subject #5). Figure 8 describes schematically the probable cascade of events in CF that leads to changes in the flow-independent parameters and little or no changes in the exhaled NO concentration as previously described.

It is important to note that asthma, or reactive airways disease, can also substantially impact NO exchange dynamics. Only two of the CF subjects (subjects #3 and #7) did not have concurrent reactive airways disease. However, these two subjects did not display remarkably different NO exchange parameters. One subject with CF had a very high $J_{NO,max}$ and $D_{NO,air}$ (subject #2). There was nothing remarkable in this subject's clinical history; however, this subject had by far the best lung function of the subjects with CF (*see* Table 1). The clinical significance of this relationship is not known.

The larger intramaneuver confidence interval in patients with CF (Figure 5) is due to the smaller lung volume (Table 1 and Figure 6), relative inhomogeneity of gas distribution, and magnitude of the exhaled NO signal. Even though the range

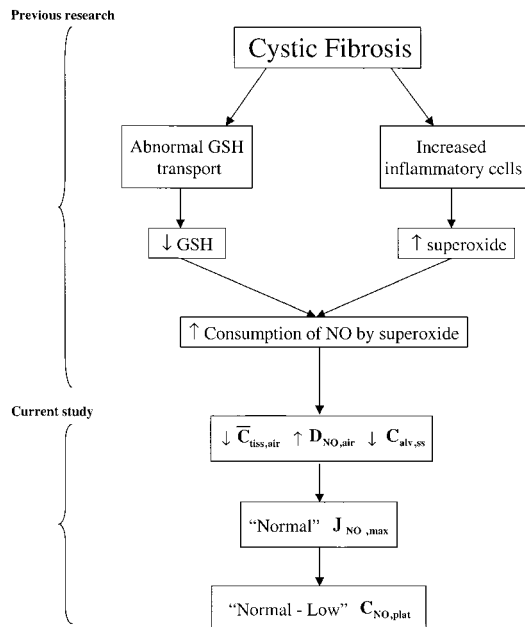


Figure 8. Schematic of the possible mechanisms underlying nitric oxide exchange dynamics in CF. A cascade of events may be initiated by abnormal GSH transport and influx of inflammatory cells, which leads to increased consumption of NO, decreased tissue phase concentration of NO, slightly decreased alveolar gas phase concentration, and increased airway diffusing capacity. This combination of changes leads to relatively normal airway flux of NO and normal to low exhaled NO concentration.

of exhalation flow rates is scaled to the lung volume, a smaller lung volume results in a smaller absolute range of sampled flow rates. Thus, the smaller exhaled volume results in a smaller change in the exhaled NO signal with changing flow rate thereby decreasing the accuracy of the parameter estimate (based on the nonlinear least-square regression technique). In addition, the absolute exhaled concentration of NO tends to be smaller in CF, which decreases the signal-to-noise ratio of the analytical instrument.

As previously described, only six of the nine children with CF were able to complete the 20-s breathhold. Although a 20-s breathhold is desirable, it is not required. We have previously reported (16) theoretically and experimentally that the uncertainty of $D_{NO,air}$ decreases as the breathhold time increases up to 20 s. The estimation of $D_{NO,air}$ depends almost exclusively on the magnitude of the peak in phase I (see Figure 6), which increases with increasing breathhold time (16).

In spite of the differences observed with CI^m , the intrasubject (CI^s) variability is not significantly different between healthy control subjects and patients with CF (see Figure 4). This finding suggests that the reproducibility of the breathing maneuver does not depend on the presence of CF despite the fact that three of the children with CF were not able to hold their breath for 20 s. Each of these three children held their breath for approximately the same length of time for each of the breathing maneuvers.

The intrapopulation (CI^p) variability did not differ between the healthy children and patients with CF, and is similar for all of the flow-independent parameters (range 46–82%). This variation within the population is much larger than other endogenous gases (e.g., CO_2). The mechanisms underlying the intrapopulation variability both in health and disease are not known, but might be related to the presence of subclinical inflammation in healthy control subjects or genetically deter-

mined differences in NO metabolism as characterized by the length of a repeated polymorphism in the neuronal nitric oxide synthase gene in patients with CF (39, 40).

There are permanent structural changes that occur in the CF lung, particularly those related to anatomic and physiological deadspace. The physiological deadspace in CF is normal to slightly increased relative to healthy control subjects (41). Thus, our estimate of the airway compartment volume (volume of airway compartment [V_{air} , ml] Table 1), which is based on the subjects ideal body weight and age, may underestimate V_{air} . We have previously shown that $D_{NO,air}$ is the most sensitive of the three flow-independent parameters to the choice of V_{air} (16). The dependence is positive; that is, as V_{air} increases, the estimate of $D_{NO,air}$ also increases to compensate for the dilutional effect of the larger volume. Thus, a slightly larger V_{air} for children with CF would actually serve to increase the $D_{NO,air}$ further from the healthy control population. Nitrogen washout is a common method to estimate anatomical deadspace; however, the accuracy of this method is compromised by the presence of diseases that impact emptying patterns. The dependence of $D_{NO,air}$ on V_{air} may explain some of the intersubject variability, and suggests that intrasubject longitudinal changes in the flow-independent parameters may have the greatest clinical utility.

Another possible source of error is performing the spirometric breathing maneuvers before the NO breathing maneuver. According to Silkoff and coworkers (42) and Deykin and coworkers (43, 44), spirometry can depress exhaled NO levels by 10–36% from the baseline in healthy subjects and subjects with asthma by an unknown mechanism. This may perturb one or more of the flow-independent parameters, and should be considered in any future studies.

In summary, we have quantified flow-independent parameters characteristic of NO exchange dynamics in the lungs of healthy children and age-matched patients with CF. The airway diffusing capacity and tissue concentration are significantly different between the two populations and may be a more effective technique than the plateau concentration in distinguishing NO exchange in patients with CF from healthy control subjects. In addition, the flow-independent parameters are not correlated with standard spirometry, which suggests that they may provide additional information to the clinician regarding the inflammatory status of the airways and alveolar region in patients with CF. Their precise interpretation will not be known until future studies establish the correlation of these parameters with more established markers of inflammation obtained by more invasive means.

Acknowledgment: The authors would like to thank the General Clinical Research Center (GCRC) at University of California, Irvine, and Dr. Eliezer Nussbaum at Miller Children's Hospital at Long Beach Memorial Medical Center for recruiting patients with CF.

References

- Gustafsson LE, Leone AM, Persson MG, Wiklund NP, Moncada S. Endogenous nitric oxide is present in the exhaled air of rabbits, guinea pigs and humans. *Biochem Biophys Res Commun* 1991;181:852–857.
- Silkoff PE, McClean PA, Caramori M, Slutsky AS, Zamel N. A significant proportion of exhaled nitric oxide arises in large airways in normal subjects. *Respir Physiol* 1998;113:33–38.
- Alving K, Weitzberg E, Lundberg JM. Increased amount of nitric oxide in exhaled air of asthmatics. *Eur Respir J* 1993;6:1368–1370.
- Lundberg JO, Weitzberg E, Lundberg JM, Alving K. Nitric oxide in exhaled air. *Eur Respir J* 1996;9:2671–2680.
- Dotsch J, Demirakca S, Terbrack HG, Huls G, Rascher W, Kuhl PG. Airway nitric oxide in asthmatic children and patients with cystic fibrosis. *Eur Respir J* 1996;9:2537–2540.
- Lundberg JO, Nordvall SL, Weitzberg E, Kollberg H, Alving K. Ex-

- haled nitric oxide in paediatric asthma and cystic fibrosis. *Arch Dis Child* 1996;75:323–326.
7. Kroesbergen A, Jobsis Q, Bel EH, Hop WC, de Jongste JC. Flow-dependency of exhaled nitric oxide in children with asthma and cystic fibrosis. *Eur Respir J* 1999;14:871–875.
 8. Thomas SR, Kharitonov SA, Scott SF, Hodson ME, Barnes PJ. Nasal and exhaled nitric oxide is reduced in adult patients with cystic fibrosis and does not correlate with cystic fibrosis genotype. *Chest* 2000;117:1085–1089.
 9. Grasemann H, Michler E, Wallot M, Ratjen F. Decreased concentration of exhaled nitric oxide (NO) in patients with cystic fibrosis. *Pediatr Pulmonol* 1997;24:173–177.
 10. Balfour-Lynn IM, Laverty A, Dinwiddie R. Reduced upper airway nitric oxide in cystic fibrosis. *Arch Dis Child* 1996;75:319–322.
 11. Corradi M, Montuschi P, Donnelly LE, Pesci A, Kharitonov SA, Barnes PJ. Increased nitrosothiols in exhaled breath condensate in inflammatory airway diseases. *Am J Respir Crit Care Med* 2001;163:854–858.
 12. Ho LP, Innes JA, Greening AP. Nitrite levels in breath condensate of patients with cystic fibrosis is elevated in contrast to exhaled nitric oxide. *Thorax* 1998;53:680–684.
 13. Ho LP, Innes JA, Greening AP. Exhaled nitric oxide is not elevated in the inflammatory airways diseases of cystic fibrosis and bronchiectasis. *Eur Respir J* 1998;12:1290–1294.
 14. Kharitonov SA, Barnes PJ. Nasal contribution to exhaled nitric oxide during exhalation against resistance or during breath holding. *Thorax* 1997;52:540–544.
 15. Grasemann H, Ratjen F. Cystic fibrosis lung disease: the role of nitric oxide. *Pediatr Pulmonol* 1999;28:442–448.
 16. Tsoukias NM, Shin HW, Wilson AF, George SC. A single-breath technique with variable flow rate to characterize nitric oxide exchange dynamics in the lungs. *J Appl Physiol* 2001;91:477–487.
 17. American Thoracic Society. Recommendations for standardized procedures for the online and offline measurement of exhaled lower respiratory nitric oxide and nasal nitric oxide in adults and children—1999. *Am J Respir Crit Care Med* 1999;160:2104–2117.
 18. Kharitonov S, Alving K, Barnes PJ. Exhaled and nasal nitric oxide measurements: recommendations. The European Respiratory Society Task Force. *Eur Respir J* 1997;10:1683–1693.
 19. Tsoukias NM, George SC. A two-compartment model of pulmonary nitric oxide exchange dynamics. *J Appl Physiol* 1998;85:653–666.
 20. Hyde RW, Geigel EJ, Olszowka AJ, Krasney JA, Forster RE 2nd, Utell MJ, Frampton MW. Determination of production of nitric oxide by lower airways of humans—theory. *J Appl Physiol* 1997;82:1290–1296.
 21. Pietropaoli AP, Perillo IB, Torres A, Perkins PT, Frasier LM, Utell MJ, Frampton MW, Hyde RW. Simultaneous measurement of nitric oxide production by conducting and alveolar airways of humans. *J Appl Physiol* 1999;87:1532–1542.
 22. Silkoff PE, Sylvester JT, Zamel N, Permutt S. Airway nitric oxide diffusion in asthma. Role in pulmonary function and bronchial responsiveness. *Am J Respir Crit Care Med* 2000;161(4, Part 1):1218–1228.
 23. Roum JH, Buhl R, McElvaney NG, Borok Z, Crystal RG. Systemic deficiency of glutathione in cystic fibrosis. *J Appl Physiol* 1993;75:2419–2424.
 24. Gao L, Kim KJ, Yankaskas JR, Forman HJ. Abnormal glutathione transport in cystic fibrosis airway epithelia. *Am J Physiol* 1999;277(1, Part 1):L113–L118.
 25. Jones KL, Bryan TW, Jinkins PA, Simpson KL, Grisham MB, Owens MW, Milligan SA, Markewitz BA, Robbins RA. Superoxide released from neutrophils causes a reduction in nitric oxide gas. *Am J Physiol* 1998;275(6, Part 1):L1120–L1126.
 26. Shin H-W, George SC. Microscopic modeling of nitric oxide and S-nitrosoglutathione kinetics and transport in human airways. *J Appl Physiol* 2001;90:777–788.
 27. Borok Z, Buhl R, Grimes GJ, Bokser AD, Hubbard RC, Holroyd KJ, Roum JH, Czerski DB, Cantin AM, Crystal RG. Effect of glutathione aerosol on oxidant-antioxidant imbalance in idiopathic pulmonary fibrosis. *Lancet* 1991;338:215–216.
 28. Roum JH, Borok Z, McElvaney NG, Grimes GJ, Bokser AD, Buhl R, Crystal RG. Glutathione aerosol suppresses lung epithelial surface inflammatory cell-derived oxidants in cystic fibrosis. *J Appl Physiol* 1999;87:438–443.
 29. Grasemann H, Gaston B, Fang K, Paul K, Ratjen F. Decreased levels of nitrosothiols in the lower airways of patients with cystic fibrosis and normal pulmonary function. *J Pediatr* 1999;135:770–772.
 30. Linnane SJ, Keatings VM, Costello CM, Moynihan JB, O'Connor CM, Fitzgerald MX, McLoughlin P. Total sputum nitrate plus nitrite is raised during acute pulmonary infection in cystic fibrosis. *Am J Respir Crit Care Med* 1998;158:207–212.
 31. Grasemann H, Ioannidis I, Tomkiewicz RP, de Groot H, Rubin BK, Ratjen F. Nitric oxide metabolites in cystic fibrosis lung disease. *Arch Dis Child* 1998;78:49–53.
 32. Jones KL, Hegab AH, Hillman BC, Simpson KL, Jinkins PA, Grisham MB, Owens MW, Sato E, Robbins RA. Elevation of nitrotyrosine and nitrate concentrations in cystic fibrosis sputum. *Pediatr Pulmonol* 2000;30:79–85.
 33. Bird RB, Stewart WE, Lightfoot EN. Transport phenomena. New York: Wiley; 1960.
 34. Kharitonov SA, Wells AU, O'Connor BJ, Cole PJ, Hansell DM, Logan-Sinclair RB, Barnes PJ. Elevated levels of exhaled nitric oxide in bronchiectasis. *Am J Respir Crit Care Med* 1995;151:1889–1893.
 35. Kharitonov SA, Yates D, Robbins RA, Logan-Sinclair R, Shinebourne EA, Barnes PJ. Increased nitric oxide in exhaled air of asthmatic patients. *Lancet* 1994;343:133–135.
 36. Kelley TJ, Drumm ML. Inducible nitric oxide synthase expression is reduced in cystic fibrosis murine and human airway epithelial cells. *J Clin Invest* 1998;102:1200–1207.
 37. Meng QH, Springall DR, Bishop AE, Morgan K, Evans TJ, Habib S, Gruenert DC, Gyi KM, Hodson ME, Yacoub MH, Polak JM. Lack of inducible nitric oxide synthase in bronchial epithelium: a possible mechanism of susceptibility to infection in cystic fibrosis. *J Pathol* 1998;184:323–331.
 38. Downey D, Elborn JS. Nitric oxide, iNOS, and inflammation in cystic fibrosis. *J Pathol* 2000;190:115–116.
 39. Wechsler ME, Grasemann H, Deykin A, Silverman EK, Yandava CN, Israel E, Wand M, Drazen JM. Exhaled nitric oxide in patients with asthma: association with NOS1 genotype. *Am J Respir Crit Care Med* 2000;162:2043–2047.
 40. Grasemann H, Knauer N, Buscher R, Hubner K, Drazen JM, Ratjen F. Airway nitric oxide levels in cystic fibrosis patients are related to a polymorphism in the neuronal nitric oxide synthase gene. *Am J Respir Crit Care Med* 2000;162:2172–2176.
 41. Lewis SM. Emptying patterns of the lung studied by multiple-breath N₂ washout. *J Appl Physiol* 1978;44:424–430.
 42. Silkoff PE, Wakita S, Chatkin J, Ansarin K, Gutierrez C, Caramori M, McClean P, Slutsky AS, Zamel N, Chapman KR. Exhaled nitric oxide after beta₂-agonist inhalation and spirometry in asthma. *Am J Respir Crit Care Med* 1999;159:940–944.
 43. Deykin A, Halpern O, Massaro AF, Drazen JM, Israel E. Expired nitric oxide after bronchoprovocation and repeated spirometry in patients with asthma. *Am J Respir Crit Care Med* 1998;157(3, Part 1):769–775.
 44. Deykin A, Massaro AF, Coulston E, Drazen JM, Israel E. Exhaled nitric oxide following repeated spirometry or repeated plethysmography in healthy individuals. *Am J Respir Crit Care Med* 2000;161(4, Part 1):1237–1240.
 45. Bouhuys A. Respiratory dead space. In: Handbook of physiology. Bethesda, MD: The American Physiological Society; 1987. p. 699–714.

APPENDIX

Model Solution

Solution of the governing differential equations for the model leads to the following governing equation for the exhaled NO concentration (16):

$$C_{\text{exh}}(t) = \left(C_{\text{alv,ss}} - \frac{J_{\text{NO,max}}}{D_{\text{NO,air}}} \right) e^{-\frac{D_{\text{NO,air}}}{V_{\text{air}}} \tau_{\text{res}}(t)} + \frac{J_{\text{NO,max}}}{D_{\text{NO,air}}} \quad (A1)$$

where V_{air} is the volume of the airway compartment and residence time of each differential gas bolus in the airway compartment (τ_{res}) is the residence time of a differential gas bolus in the airway compartment. V_{air} (ml) is approximated by the physiological dead space, which is derived by subject age in years plus ideal body weight in pounds (45). Equation A1 is compared with the experimental data and used to estimate the three remaining unknown parameters ($J_{\text{NO,max}}$, $D_{\text{NO,air}}$, and $C_{\text{alv,ss}}$) using nonlinear least-squares regression. Once values for $J_{\text{NO,max}}$, $D_{\text{NO,air}}$, and $C_{\text{alv,ss}}$ are known, Equation A1 can be used to predict the exhalation curves presented in Figure 6 or to predict the $C_{\text{NO,plat}}$ at a constant exhalation flow rate (Table 2).

Airway Diffusing Capacity

It has been previously shown that $D_{\text{NO,air}}$ can theoretically be approximated by the following expression:

$$D_{\text{NO,air}} = \frac{A_{\text{air}} \lambda_{\text{tiss,air}} \sqrt{\mathcal{D}_{\text{NO,tiss}} k}}{\tanh(\xi)} \quad (A2)$$

where $\lambda_{\text{tiss:air}}$ is the tissue:air partition coefficient, k (s^{-1}) is the first-order rate constant that characterizes the rate of chemical consumption by substrates such as superoxide, airway surface area available for NO diffusion (cm^2) (A_{air}) is the surface area

available for diffusion, molecular diffusivity of NO in the tissue ($\mathcal{D}_{\text{NO,tiss}}$) (cm^2/s) is the molecular diffusivity of NO in the tissue, $\xi = L_{\text{tiss}}/\sqrt{\mathcal{D}_{\text{NO,tiss}}/k}$, and thickness of the tissue layer (cm) (L_{tiss}) is the thickness of the tissue layer. The hyperbolic tangent (\tanh) is bounded between -1 and 1 , and is a monotonically increasing function of its argument. From Equation A2, $D_{\text{NO,air}}$ is a positive function of A_{air} , $\lambda_{\text{tiss:air}}$, $\mathcal{D}_{\text{NO,tiss}}$, and k , and is an inverse function of L_{tiss} . Values of A_{air} , $\lambda_{\text{tiss:air}}$, $\mathcal{D}_{\text{NO,tiss}}$, and L_{tiss} are $9,100 \text{ cm}^2$, 0.0412 , $3.3 \times 10^{-5} \text{ cm}^2/\text{s}$, and 0.01 cm as previously reported (16, 19). Equation A2 provides units of ml/s for $D_{\text{NO,air}}$ that are equivalent to $\text{pl s}^{-1} \text{ ppb}^{-1}$.